Rough-Wall Turbulent Heat Transfer with Step-Wall Temperature Boundary Conditions

Robert P. Taylor,* M. H. Hosni,† James W. Garner,‡ and Hugh W. Coleman§
Mississippi State University, Mississippi State, Mississippi 39762

Stanton number measurements are presented for the turbulent boundary layer flow of air on rough-wall flat plates with both constant wall temperature and step wall temperature boundary conditions. Two rough surfaces were used—one roughened with hemispheres spaced four diameters apart and the other with hemispheres spaced two diameters apart. The data are compared with each other and with results from a smooth surface tested in the same experimental facility. It is found that, when plotted as the ratio of Stanton number to constant wall temperature Stanton number vs the ratio of unheated length to distance from the leading edge, the data from the smooth and rough surfaces scatter about a single curve. This gives a new kernel function that, when used in the superposition solution of the arbitrary wall temperature problem, yields good results for both smooth and rough surfaces.

Nomenclature

A = plate plan area
C_p = freestream specific heat
c_i = step temperature strength
d_0 = roughness element base diameter
L = roughness element spacing
P_{bar} = barometric pressure
Pr = Prandtl number
q_c = conductive heat loss rate
q_r = radiative heat loss rate
Re_x = Reynolds number based on x
r = recovery factor
St = Stanton number
St_t = Stanton number for constant wall temperature
T_0 = freestream total temperature
T_r = recovery temperature
T_{rail} = rail temperature
T_w = wall temperature
T_{wb} = wet bulb temperature
U_∞ = freestream velocity
$(UA)_{eff}$ = effective overall conductance for q_c
W = plate heater power
x = longitudinal coordinate from nozzle exit
x_T = total length
α = parameter in curve-fit formula
γ = parameter in curve-fit formula
$\Delta T(x)$ = temperature difference $T_w - T_0$
ϵ = emissivity
ρ = density
ϕ = unheated length

Received Dec. 14, 1989; revision received March 19, 1990; presented as Paper 90-1501 at the AIAA 21st Fluid Dynamics, Plasmadynamics, and Lasers Conference, Seattle, WA, June 18-20, 1990.

*Associate Professor, Thermal and Fluid Dynamics Laboratory, Mechanical and Nuclear Engineering Department. Member AIAA.

†Research Associate, Thermal and Fluid Dynamics Laboratory, Mechanical and Nuclear Engineering Department. Member AIAA.

‡Graduate Student, Thermal and Fluid Dynamics Laboratory, Mechanical and Nuclear Engineering Department.

§Professor, Thermal and Fluid Dynamics Laboratory, Mechanical and Nuclear Engineering Department. Member AIAA.

Introduction

STANTON number measurements with constant wall temperature and step wall temperature boundary conditions are presented for turbulent flow of air over rough plates. The step wall temperature case is one of the fundamental problems of convective heat transfer. Under the assumption of incompressible flow with constant fluid properties, the problem of heat transfer in the boundary layer with arbitrary thermal boundary condition becomes amenable to solution by superposition. The simplest boundary condition for which solutions can serve as kernel functions for this superposition is the step wall temperature. Thus, once the influence of a step change in wall temperature on the boundary layer heat transfer is understood, the problem of arbitrary thermal boundary condition is solved. The step wall temperature case is also of practical interest. It occurs often in atmospheric flows, such as the land-sea interface and in heat exchangers.

Because of its fundamental importance and probably because it is one of the easier heat transfer experiments to construct, there has been a large amount of work reported in the literature for boundary layer heat transfer with a step wall temperature boundary condition on smooth surfaces. Jakob and Dow[1] studied the effect of unheated starting length for turbulent airflow parallel to a circular cylinder. They measured the average Nusselt number based on total cylinder length for a variety of cases and obtained a relationship for $Nu_L = f(Re_L)$. By differentiating this result, they obtained a relationship for the local heat transfer that can be expressed as

$$\frac{St}{St_t} = 0.8 + 0.2\left(\frac{\phi}{x}\right) - 0.78\left(\frac{\phi}{x}\right)^{2.75} + 1.18\left(\frac{\phi}{x}\right)^{3.75} \tag{1}$$

The maximum Reynolds number for their work was about 1,500,000. Tessin and Jakob[2] reported additional measurements on cylinders with maximum Reynolds numbers of about 2,500,000. Maisel and Sherwood[3] obtained turbulent mass transfer data with a variety of starting lengths on a plate, and empirically determined a formula for average mass transfer rates that (using the heat transfer analogy) is equivalent to

$$\frac{\overline{St}}{\overline{St_t}} = \left[1 - \left(\frac{\phi}{x_T}\right)^{0.8}\right]^{-0.11} \tag{2}$$

where the overbar indicates averaged values.

The problem of the step wall temperature boundary condition has also received considerable theoretical treatment for smooth surfaces. Rubesin[4] developed an analysis using the integral boundary layer equations and the 1/7-power law ap-

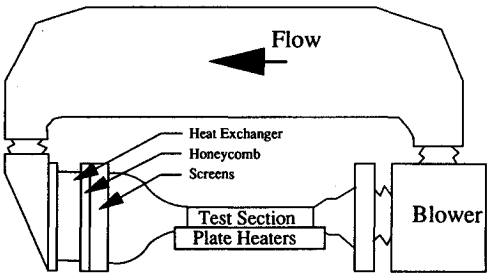

Fig. 1 Schematic of the turbulent heat transfer test facility (THTTF).

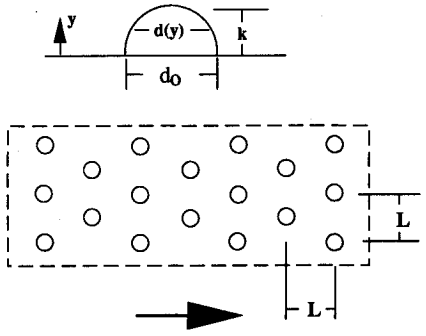

Fig. 2 Surface roughness geometry.

proximations for the boundary layer velocity and temperature profiles. He arrived at a semiempirical formula that, when adjusted to fit Scesa's[5] data for step wall temperature on a flat plate, gave

$$\frac{St}{St_t} = \left[1 - \left(\frac{\phi}{x}\right)^{39/40}\right]^{-7/39} \tag{3}$$

Reynolds et al.[6] also performed an analysis using the integral boundary-layer equations and the 1/7-power law approximations and arrived at the formula

$$\frac{St}{St_t} = \left[1 - \left(\frac{\phi}{x}\right)^{9/10}\right]^{-1/9} \tag{4}$$

They conducted extensive experiments, running some 18 different step wall temperature cases with Reynolds numbers ranging up to 3,500,000, which compared well with Eq. (4). They also performed experiments with arbitrary wall temperatures and applied Eq. (4) through the superposition solution with good results. Spalding[7] performed an analysis using results from numerical solutions of the Reynolds-averaged boundary layer equations and arrived at a rather complicated but more general formula, which Rubesin and Inouye[8] showed to reduce to Eq. (4) for air after a short distance downstream from the step.

More recently, measurements have been reported by Antonia et al.[9] for turbulent boundary layer flow with an unheated length followed by a region of constant heat flux. They found that the superposition solution using Eq. (4) as the kernel was in reasonable agreement with their Stanton number measurements. Saetran[10] measured the development of the thermal boundary layer downstream of a step change in wall temperature. He found Spalding's formula to be in good agreement with his Stanton number data. Taylor et al[11] measured Stanton number distributions in turbulent boundary layers with unheated lengths followed by either a constant wall temperature or a constant heat flux for Reynolds numbers up to 10,000,000. They found Eq. (4) to be a reasonable representation of their data.

The current general consensus in textbooks and handbooks (Pletcher,[12] Rubesin and Inouye,[8] and Cebeci and Bradshaw,[13] for example) is that Eq. (4) is the proper formula for use as the kernel in the superposition solution for turbulent boundary layer flow over smooth surfaces.

Rough surfaces have received less attention. Coleman[14] and Coleman et al.[15] studied the effects of step wall temperature and other nonuniform wall temperature boundary conditions on heat transfer in the turbulent boundary layer over a surface roughened with 1.27-mm-diam spheres packed in the most dense array. They proposed the formula

$$\frac{St}{St_t} = \left[1 - \left(\frac{\phi}{x}\right)\right]^{-0.22} \tag{5}$$

When this formula was used in the superposition solution, reasonable agreement was found with the nonuniform wall temperature cases. Ligrani[16] studied heat transfer in artificially thickened boundary layers over the same surface as Coleman. Because of the apparent origin of his momentum boundary layer, his data have effects of an unheated starting length.

The experiments reported in this paper were designed to investigate the effects of the step wall temperature boundary condition on heat transfer in the turbulent rough-wall boundary layer for Re_x approaching 10,000,000. All data are for airflow with a constant freestream velocity and temperature over a 2.4-m-long flat plate. Two rough surfaces were used. The first was a smooth plate roughened with 1.27-mm-diam hemispheres uniformly spaced four base diameters apart ($L/d_0 = 4$) in a staggered array. The second surface was the same but with hemispheres spaced two diameters apart ($L/d_0 = 2$). A variety of unheated length cases and freestream velocities were considered. Also, previously reported data from Love et al.[17] for a smooth surface in the same facility and data from Coleman[14] for a rough surface in a different but similar facility are included. This gives a data set that contains aerodynamically smooth, transitionally rough, and fully rough flow cases. The step temperature boundary condition data are used to obtain a new kernel function. Results using this kernel function in the superposition solution are compared with Stanton number data from arbitrary wall temperature experiments for both smooth and rough surfaces with good agreement.

Experimental Apparatus and Measurement Procedures

The experiments were performed in the turbulent heat transfer test facility (THTTF), which is shown schematically in Fig. 1. Complete descriptions of the facility and its qualification are presented in Coleman et al.[18] This facility is a closed-loop wind tunnel with a freestream velocity range of 6–67 m/s. The temperature of the circulating air is controlled with an air to water heat exchanger and a cooling water loop. Following the heat exchanger, the airflow is conditioned by a system of honeycomb and screens.

The bottom wall of the 2.4-m-long by 0.5-m-wide by 0.1-m-high test section consists of 24 electrically heated flat plates that are abutted together to form a continuous flat surface. The allowable step or mismatch between any two plates is 0.013 mm. Each nickel-plated aluminum plate (about 10 mm thick by 0.1 m in the flow direction) is uniformly heated from below a custom-manufactured, rubber-encased electric heater pad. Design computations showed that, with this configuration, a plate can be considered to be at a uniform temperature. The heating system is under active computer control, and any desired set of plate temperatures can be maintained within the limits of the power supply. For example, the plate temperature can be maintained at any temperature ±0.1°C between 50°C and 2°C above the freestream air temperature, which is typically 30°C. To minimize the conduction losses, the side rails

that support the plates are maintained at approximately the same temperature as the plates.

The top wall can be adjusted to achieve a constant freestream velocity. An inclined water manometer with a resolution of 0.06 mm is used to measure the pressure gradient during top wall adjustment. Static pressure taps are located in the side wall adjacent to each plate. The pressure tap located at the second plate is used as a reference, and the pressure difference between it and each other tap is minimized. For example, the maximum pressure difference for a freestream velocity of 43 m/s was 0.30 mm of water.

The boundary layer is tripped at the exit of the 19:1 area ratio nozzle with a 1 × 12 mm wooden strip. This trip location is immediately in front of the heated surface.

Three separate sets of surface plates were used in the experiments discussed here—one smooth and two rough. The smooth plates have a measured average roughness of less than 0.5 μm. Therefore, they are both visually and aerodynamically smooth. Each rough plate was precision-machined from a solid piece of aluminum using a specially designed diamond tool. A precision numerical milling machine was used to mill out an array of cubes. The special diamond tool was then used to form the cubes into hemispheres. The finished plates were then nickel plated. The result was a very smooth flat surface with a staggered array of hemispherical roughness elements, with base diameter $d_0 = 1.27$ mm, as shown in Fig. 2. The measured average roughness on the "smooth" wall portion of the plates with $L/d_0 = 4$ is less than 1.6 μm. The surface finish on the plates with $L/d_0 = 2$ is visually smooth—the same appearance as the other surfaces. However, the finish was not measured because the available profilometer stylus would not fit between the rows.

Since the roughness elements and the base plate are a continuous piece of aluminum, the thermal contact between the elements and the base is perfect. For the conditions of these experiments, design calculations showed that each plate and its roughness elements can be considered to be at a uniform temperature.

Before proceeding with the testing, a series of smooth-wall qualification tests were performed to insure the fitness of the test rig and the correctness of the instrumentation and the data acquisition and reduction procedures.[18] Measurements in the nozzle exit plane showed the mean velocity to be uniform within about 0.5% and the freestream turbulence intensity to be less than 0.3%. Measurements 1.1 m downstream of the nozzle exit showed the spanwise variation of the momentum thickness to be less than ±5%. Profiles of mean temperature and velocity were in good agreement with the usual "laws-of-the-wall." Stanton number data for the constant wall temperature cases were in excellent agreement with the data of Reynolds et al.,[6] which is the definitive data set on which the usual Stanton number correlations are based. The THTTF smooth-wall data fall within the data scatter of this definitive data set.

Stanton Number Determination

The data reduction expression for the experimentally determined Stanton number is

$$St = \frac{W - q_r - q_c}{A\rho C_p U_\infty (T_w - T_0)} \tag{6}$$

The power W supplied to each plate heater is measured with a precision wattmeter. The radiation heat loss q_r is estimated using a gray body enclosure model where the emissivity of the nickel-plated aluminum is estimated as $\epsilon = 0.11$. The conductive heat loss q_c is calculated using an experimentally determined effective plate conductance $(UA)_{\text{eff}}$, which includes both side rail and back losses. The conduction losses are minimized by actively heating the side rails. Both q_r/W and q_c/W are generally in the 0.5–1% range. The plate area A is determined from the length and width dimensions. The density and specific heat are determined from property data for moist air using the measured values of barometric pressure and wet and dry bulb temperatures in the tunnel. The freestream velocity is measured using a pitot probe and specially calibrated precision pressure transducers. The freestream and plate temperatures are measured using specially calibrated thermistors. The freestream total temperature T_0 is computed using the measured freestream recovery temperature T_r and a recovery factor for the freestream thermistor probe of $r = 0.86$.[19] The plate temperatures T_w are measured using two thermistors installed in wells in the back of each plate using conducting paste. All fluid properties are evaluated at the freestream static temperature.

The experimentally determined Stanton number is then a function of the 13 measured variables and reference parameters:

$$St = St[W, \epsilon, A, T_w, T_r, T_{\text{rail}}, (UA)_{\text{eff}}, T_{wb}, P_{\text{bar}}, C_{\text{pair}}, C_{p\text{water}}, U_\infty, r] \tag{7}$$

The uncertainty in the experimental Stanton number was estimated based on the American National Standards Institute/American Society of Mechanical Engineers Standard on measurement uncertainty[20] following the procedures of Coleman and Steele.[21] For the experiments reported in this paper, precision errors associated with all measured variables used to determine the Stanton number were found to be negligible compared with the corresponding bias errors. For the Stanton number data in this paper, the overall uncertainty, as discussed in detail in Coleman et al.,[18] ranged from about 2 to 5%, depending on flow conditions.

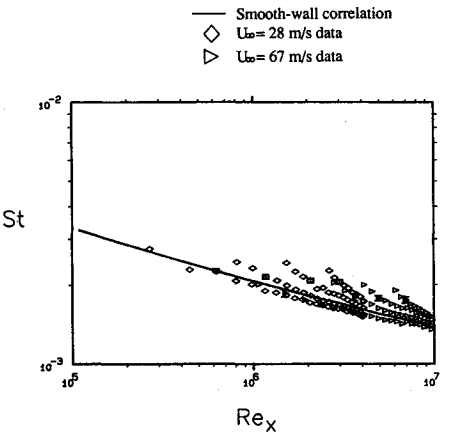

Fig. 3 Plot of the Stanton number data for the smooth surface.

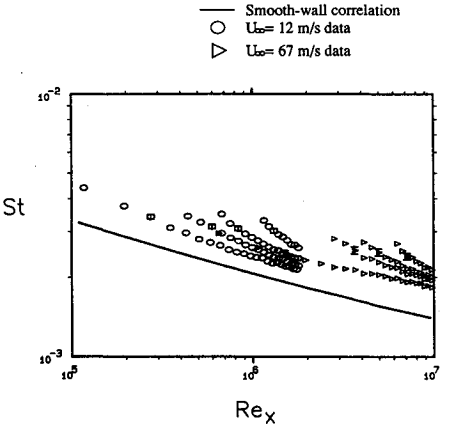

Fig. 4 Plot of the Stanton number data for the rough surface with $L/d_0 = 4$.

Table 1 Summary of step temperature test conditions

	Unheated length						
Surface—U_∞, m/s	0.0 m	0.3 m	0.4 m	0.5 m	0.7 m	0.8 m	1.3 m
Smooth—28	X	X	—	—	X	—	X
Smooth—67	X	—	—	X	—	X	X
$L/d_0=4$—12	X	—	X	—	X	—	X
$L/d_0=4$—67	X	—	—	X	—	X	X
$L/d_0=2$—12	X	—	X	—	X	—	X
$L/d_0=2$—28	X	X	—	—	X	—	X
$L/d_0=2$—67	X	—	—	X	—	X	X

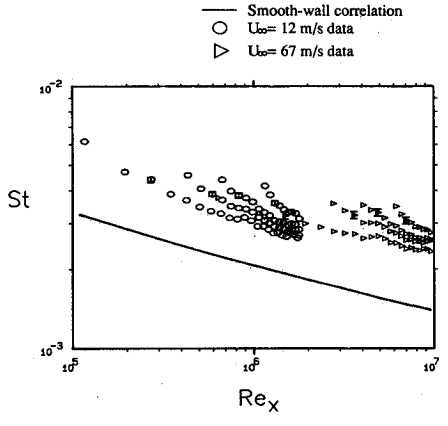

Fig. 5 Plot of the Stanton number data for the rough surface with $L/d_0=2$.

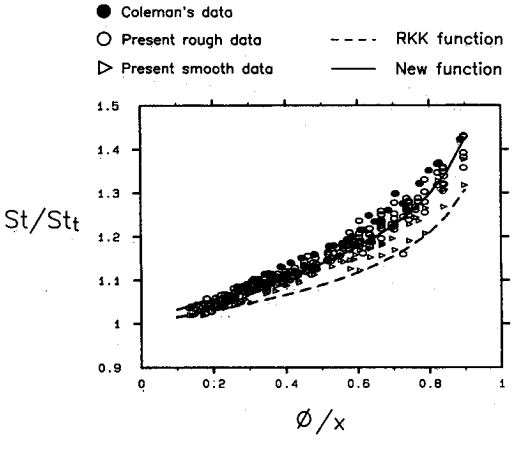

Fig. 6 Plot of the Stanton number ratio.

The Stanton numbers that are measured in this way are the average values over each 0.1 m plate. In the turbulent boundary layer, these values are excellent approximations of the local Stanton number evaluated at the plate centerline for all plates but the first heated plate, which is in all cases considered to be a guard heater in these experiments.

Stanton number ratio St/St_t, where St_t is the constant wall temperature Stanton number, is used in this paper for comparison of the experimental data and the theoretical solutions. Because the same equipment is used to measure both St and St_t, many of the bias limits involved in the uncertainty calculations of St/St_t are correlated. The effect of the correlated biases is to reduce the uncertainty in the ratio to less than 2% for all cases except the first and last heated plates, which are considered guard heaters. Data taken from these plates are not appropriately corrected for conduction losses and are not plotted in the figures.

Results and Discussion

Stanton number measurements are reported for the three surfaces with a variety of unheated lengths and freestream velocities. Table 1 summarizes the experimental conditions. The smooth-wall data were taken from previously published work.[11,17] The rough-wall data are reported for the first time here. The smooth-wall cases are, of course, aerodynamically smooth flows. For the cases with a surface roughened with hemispheres spaced four base diameters apart, Hosni[22] shows that the 12-m/s cases correspond to transitionally rough flow, and the 67-m/s cases correspond to fully rough flow. For the cases with $L/d_0=2$, Hosni shows that the 12-, 28-, and 67-m/s cases all correspond to fully rough flow.

Figure 3 shows the smooth-wall results for isothermal and step temperature boundary conditions plotted as Stanton number vs x Reynolds number, where x is measured from the nozzle exit. The different experimental cases correspond to the different unheated starting lengths as given in Table 1. The curve corresponds to the isothermal smooth-wall correlation.[23]

$$St_t = 0.185Pr^{-0.4}[\log_{10}(Re_x)]^{-2.584} \quad (8)$$

The step wall temperature data behave as expected, with the Stanton number high near the origin of the thermal layer and converging with the isothermal case as the thermal layer develops. Uncertainty bars are drawn on selected data points—the uncertainty limits correspond roughly with the symbol size.

Figure 4 shows both the isothermal and the different step temperature boundary condition (Table 1) results for the $L/d_0=4$ rough surface plotted as Stanton number vs x Reynolds number for freestream velocities of 12 and 67 m/s. The rough wall has different thermal behavior than the smooth wall. The cases with freestream velocities of 12 m/s and 67 m/s are on distinctly different tracks in these coordinates. This has been observed by others (Coleman[14] and Ligrani,[16] for example) and is the expected behavior for rough surfaces. Figure 5 shows a similar plot for the rough surface with $L/d_0=2$. As before, the uncertainty bars are plotted on selected points in the figures, with the symbol size roughly equal to the uncertainty interval. Figures 4 and 5 show that the influence of the roughness on the Stanton number is large. For the surface with $L/d_0=4$, the increase in St over the equivalent smooth-wall case is about 40%, and for $L/d_0=2$, the increase is about 75%.

Figures 3–5 indicate that the step wall temperature boundary condition has about the same effect on a Stanton number relative to the isothermal cases for all three surfaces. Figure 6 makes this comparison directly. Also included in this figure are data from two step temperature cases reported by Coleman[14] from measurements made in turbulent flat plate flow over a surface roughened with 1.27-mm-diam spheres packed in the most dense array. The data from the smooth surface and three rough surfaces group well together in these coordinates, and the smooth, transitionally rough, and fully rough

cases from the three different rough surfaces show a similar behavior. As seen in the figure, the data scatter is about ±5% near the step ($\phi/x \approx 0.8$) and about ±2% further down from the step ($\phi/x \approx 0.2$). The dashed curve in Fig. 6 corresponds to Eq. (4), which is representative of the smooth-wall data of Reynolds et al.[6] The solid curve is a curve-fit of the data as discussed below.

Since the data from the smooth surface and three rough surfaces group together so well, it was logical to derive a statistical model from this data using curve-fit procedures. Postulating a formula of the same form as Eq. (4), a chi-square minimization was performed using the Levenberg-Marquardt method as described by Press et al.[24] This resulted in the formula

$$\frac{St}{St_t} = \left[1 - \left(\frac{\phi}{x}\right)^{0.677}\right]^{-0.13} \tag{9}$$

which is plotted in Fig. 6 as the solid curve.

Equation (9) could possibly be used as a replacement for Eq. (4) as the kernel function in the superposition solution for variable wall temperature problems, since it has the advantage of representing data for both smooth and rough surfaces over the aerodynamically smooth, transitionally rough, and fully rough flow regimes. Fortunately, variable wall temperature data from both smooth and rough surfaces are available for comparison, and such comparisons are the ultimate test of proposed kernel functions.

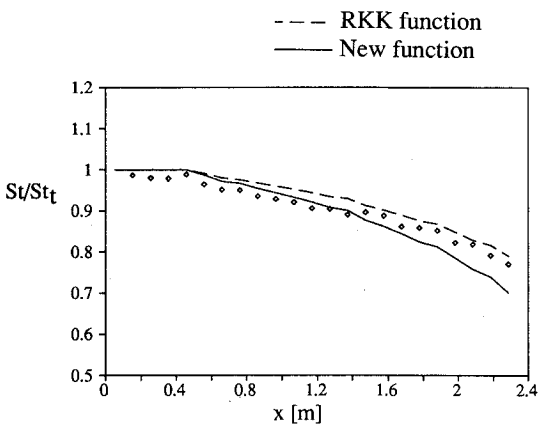

Fig. 7 Comparison of the superposition solution using both kernel functions with the smooth-wall linear temperature variation data $U_\infty = 67$ m/s from Love et al.[17]

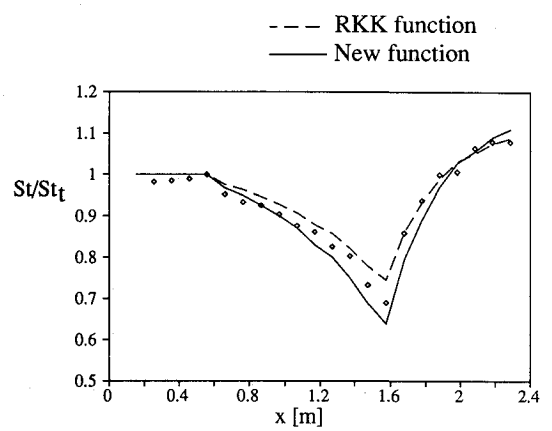

Fig. 8 Comparison of the superposition solution using both kernel functions with the smooth-wall bilinear temperature variation data $U_\infty = 67$ m/s from Love et al.[17]

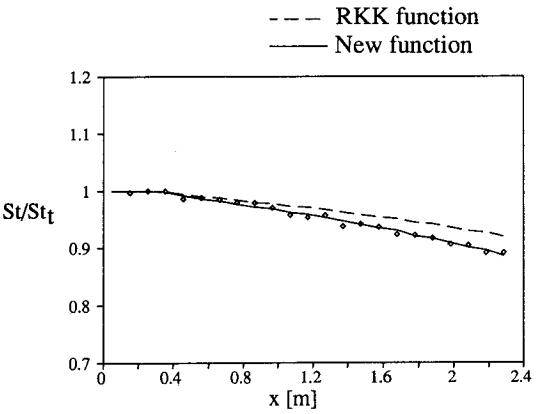

Fig. 9 Comparison of the superposition solution using both kernel functions with the rough-wall linear temperature variation data $U_\infty = 27$ m/s from Coleman et al.[14]

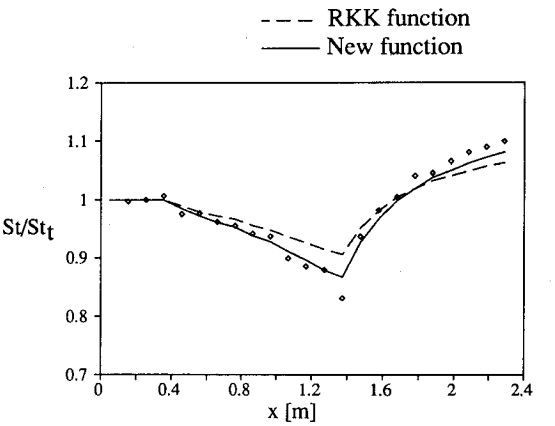

Fig. 10 Comparison of the superposition solution using both kernel functions with the rough-wall bilinear temperature variation data $U_\infty = 27$ m/s from Coleman et al.[14]

For a wall temperature distribution that is composed of a series of steps in temperature c_i, the superposition solution yields

$$\frac{St}{St_t} = \frac{1}{\Delta T(x)} \sum_{i=1}^{N} c_i \left[1 - \left(\frac{\phi_i}{x}\right)^{\gamma}\right]^{-\alpha} \tag{10}$$

This solution is compared with data from two smooth-wall and four rough-wall cases below.

Figures 7 and 8 show this comparison with smooth-wall data from Love et al.[17] Figure 7 shows the comparison for a case where the wall temperature was decreasing in a series of nominally 0.5°C steps. Figure 8 shows a similar case where the wall temperature decreases and then increases in a series of nominally 1°C steps. In both cases the measured values of the step strength c_i were used for the computations with Eq. (10). The figures show that both kernel functions give reasonable agreement with this smooth-wall data. All of the computations are within about 5% of the data, with the largest difference being about 8%. In Fig. 7, the solutions using the new function indicate a stronger response to the wall temperature variation than the solutions using the Reynolds-Kays-Kline (RKK) function. The data are in better agreement with the new function solutions for the first half of the ramp but in better agreement with the RKK function solutions for the last half of the ramp. A similar situation is seen for the bilinear wall temperature case in Fig. 8.

Figures 9 and 10 show this comparison with rough-wall data from Coleman.[14] This is the same surface discussed before that was roughened with 1.27-mm spheres packed in the most

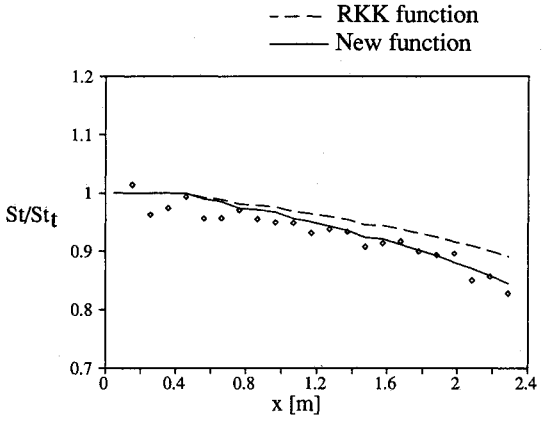

Fig. 11 Comparison of the superposition solution using both kernel functions with the rough-wall linear temperature variation data for the $L/d_0 = 4$ surface, $U_\infty = 12$ m/s.

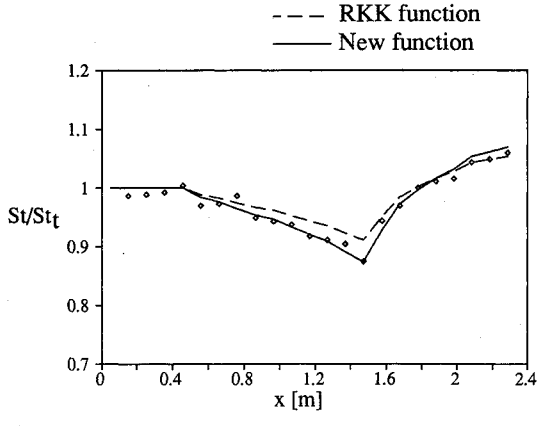

Fig. 12 Comparison of the superposition solution using both kernel functions with the rough-wall bilinear temperature variation data for the $L/d_0 = 4$ surface, $U_\infty = 67$ m/s.

dense array. According to Coleman, the boundary layer was fully rough in both cases. Figure 9 shows the comparison for a case where the wall temperature was decreased in a series of nominally 0.4°C steps. Figure 10 shows a similar comparison where the wall temperatures decreased and then increased in a series of nominally 0.8°C steps. Again, the measured values of c_i were used for the computations. The figures show that the new function yields better agreement than Eq. (4) for this rough surface.

Figures 11 and 12 show the comparison with rough-wall data taken on the present surface with $L/d_0 = 4$. Figure 11 shows the comparison for a case where the wall temperature was decreasing in a series of nominally 0.5°C steps with a freestream velocity of 12 m/s. According to Hosni,[22] this case was transitionally rough. Figure 12 shows a case where the wall temperature decreases and then increases in a series of nominally 0.5°C steps with a freestream velocity of 67 m/s. According to Hosni, this case is fully rough. Again, in both cases the measured values of the step strength c_i were used in the computations. The figures show that overall the new function yields better agreement than Eq. (4) for these cases.

Summary and Conclusions

The step wall temperature Stanton number data for turbulent flat plate boundary layer flow over a smooth surface and three rough surfaces collapse well together when plotted as St/St_t vs ϕ/x. A new function is statistically derived using nonlinear chi-square curve-fit procedures on these data. This function is shown to give good to excellent agreement with variable wall temperature Stanton number ratio data when it is used as the kernel function in the superposition solution for smooth-wall cases and transitionally rough and fully rough rough-wall cases. Based on the comparisons presented, the new function should be considered as a viable alternative to Eq. (4), which was developed solely for smooth-wall flows.

Acknowledgments

This work was supported by the U.S. Air Force Office of Scientific Research (AFOSR) (Research Grant AFOSR-86-0178); the experimental apparatus was acquired under Grant AFOSR-85-0075. The authors gratefully acknowledge the interest and encouragement of Hank Helin of AFOSR.

References

[1]Jakob, M., and Dow, W. M., "Heat Transfer from a Cylindrical Surface to Air in Parallel Flow With and Without Unheated Starting Sections," *Transactions of the ASME*, Vol. 68, No. 2, 1946, pp. 123-134.

[2]Tessin, W., and Jakob, M., "Influence of Unheated Starting Sections on Heat Transfer from a Cylinder to Gas Streams Parallel to the Axis," *Transactions of the ASME*, Vol. 75, No. 4, 1953, pp. 473-481.

[3]Maisel, D. S., and Sherwood, T. K., "Evaporation of Liquids into Turbulent Gas Streams," *Chemical Engineering Progress*, Vol. 46, No. 3, 1950, pp. 131-138.

[4]Rubesin, M. W., "The Effect of an Arbitrary Surface-Temperature Variation Along a Flat Plate on the Convective Heat Transfer in an Incompressible Turbulent Boundary Layer," NACA TN-2345, April 1951.

[5]Scesa, S., "Experimental Investigation of Convective Heat Transfer to Air from a Flat Plate with Stepwise Discontinuous Surface Temperature," M.S. Thesis, Dept. of Mechanical Engineering, Univ. of California, Berkeley, Berkeley, CA, 1951.

[6]Reynolds, W. C., Kays, W. M., and Kline, S. J., "Heat Transfer in the Turbulent Incompressible Boundary Layer," Pts. 1-3, NASA Memo 12-1-58W, 12-2-58W, 12-3-58W, Dec. 1958.

[7]Spalding, D. B., "Contribution to the Theory of Heat Transfer Across a Turbulent Boundary Layer," *International Journal of Heat Mass Transfer*, Vol. 7, No. 7, 1964, pp. 743-761.

[8]Rubesin, M. W., and Inouye, M., "Forced Convection, External Flows," *Handbook of Heat Transfer*, edited by W. M. Rohsenow and J. P. Hartnett, McGraw-Hill, New York, 1973, Chap. 8.

[9]Antonia, R. A., Danh, H. Q., and Prabhu, A., "Response of a Turbulent Boundary Layer to a Step Change in Surface Heat Flux," *Journal of Fluid Mechanics*, Vol. 80, Pt. 1, 1977, pp. 153-177.

[10]Saetran, L. R., "Turbulent Boundary Layer with a Step in Wall Temperature," *Forum on Turbulent Flows-1989*, FED-Vol. 76, edited by W. W. Bower and M. J. Morris, American Society of Mechanical Engineers, New York, 1989, pp. 107-114.

[11]Taylor, R. P., Love, P. H., Coleman, H. W., and Hosni, M. H., "The Effects of Step Changes in Thermal Boundary Condition on Heat Transfer in the Incompressible Flat Plate Turbulent Boundary Layer," *Heat Transfer in Convective Flows*, HTD-Vol. 107, edited by R. K. Shah, American Society of Mechanical Engineers, New York, 1989, pp. 9-16.

[12]Pletcher, R. H., "External Flow Forced Convection," *Handbook of Single-Phase Convective Heat Transfer,* edited by S. Kakac, R. K. Shah, and W. Aung, Wiley, New York, 1987, Chap. 2.

[13]Cebeci, T., and Bradshaw, P., *Physical and Computational Aspects of Convective Heat Transfer*, Springer-Verlag, New York, 1984.

[14]Coleman, H. W., "Momentum and Energy Transport in the Accelerated Fully Rough Turbulent Boundary Layer," Ph.D. Dissertation, Mechanical Engineering Dept., Stanford Univ., Stanford, CA, 1976; also Rept. HMT-24, 1976.

[15]Coleman, H. W., Pimenta, M. M., and Moffat, R. J., "Rough-Wall Turbulent Heat Transfer with Variable Velocity, Wall Temperature, and Blowing," *AIAA Journal*, Vol. 16, No. 1, 1978, pp. 78-82.

[16]Ligrani, P. M., "The Thermal and Hydrodynamic Behavior of Thick, Rough-Wall, Turbulent Boundary Layers," Ph.D. Dissertation, Mechanical Engineering Dept., Stanford Univ., Stanford, CA, 1979; also Rept. HMT-29, 1979.

[17]Love, P. H., Taylor, R. P., Coleman, H. W., and Hosni, M. H., "Effects of Thermal Boundary Condition on Heat Transfer in the Turbulent Incompressible Flat Plate Boundary Layer," Mechanical and Nuclear Engineering Dept., Mississippi State Univ., Rept. TFD-88-3, Mississippi State, MS, 1988.

[18]Coleman, H. W., Hosni, M. H., Taylor, R. P., and Brown, G. B., "Smooth Wall Qualification of a Turbulent Heat Transfer Test Facility," Mechanical and Nuclear Engineering Dept., Mississippi State Univ., Rept. TFD-88-2, Mississippi State, MS, 1988.

[19]Eckert, E. R. G., and Goldstein, R. J., *Measurements in Heat Transfer*, 2nd ed., McGraw-Hill, New York, 1976.

[20]Anon., *Measurement Uncertainty*, ANSI/ASME PTC 19.1-1985 Pt. 1, American Society of Mechanical Engineers, New York, 1986.

[21]Coleman, H. W., and Steele, W. G., *Experimentation and Uncertainty Analysis for Engineers*, Wiley, New York, 1989.

[22]Hosni, M. H., "Measurement and Calculation of Surface Roughness Effects on Turbulent Flow and Heat Transfer," Ph.D. Dissertation, Mechanical and Nuclear Engineering Dept., Mississippi State Univ., Mississippi State, MS, 1989; also Rept. TFD-89-1, 1989.

[23]Taylor, R. P., Coleman, H. W., Hosni, M. H., and Love, P. H., "Thermal Boundary Condition Effects on Heat Transfer in the Turbulent Incompressible Flat Plate Boundary Layer," *International Journal of Heat Mass Transfer*, Vol. 32, No. 6, 1989, pp. 1164–1174.

[24]Press, W. H., Flannery, B. P., Teukolsky, S. A., and Vetterling, W. T., *Numerical Recipes*, Cambridge Univ. Press, New York, 1986.